Accepted Manuscript

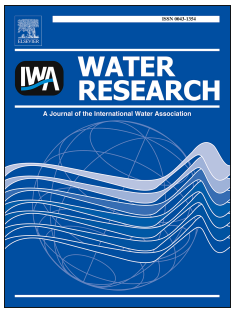

Biodegradability of DBP precursors after drinking water ozonation

Glen Andrew De Vera, Jurg Keller, Wolfgang Gernjak, Howard Weinberg, Maria José Farré

PII: S0043-1354(16)30772-2

DOI: 10.1016/j.watres.2016.10.022

Reference: WR 12420

To appear in: *Water Research*

Received Date: 29 July 2016

Revised Date: 6 October 2016

Accepted Date: 7 October 2016

Please cite this article as: De Vera, G.A., Keller, J., Gernjak, W., Weinberg, H., Farré, M.J., Biodegradability of DBP precursors after drinking water ozonation, *Water Research* (2016), doi: 10.1016/j.watres.2016.10.022.

This is a PDF file of an unedited manuscript that has been accepted for publication. As a service to our customers we are providing this early version of the manuscript. The manuscript will undergo copyediting, typesetting, and review of the resulting proof before it is published in its final form. Please note that during the production process errors may be discovered which could affect the content, and all legal disclaimers that apply to the journal pertain.

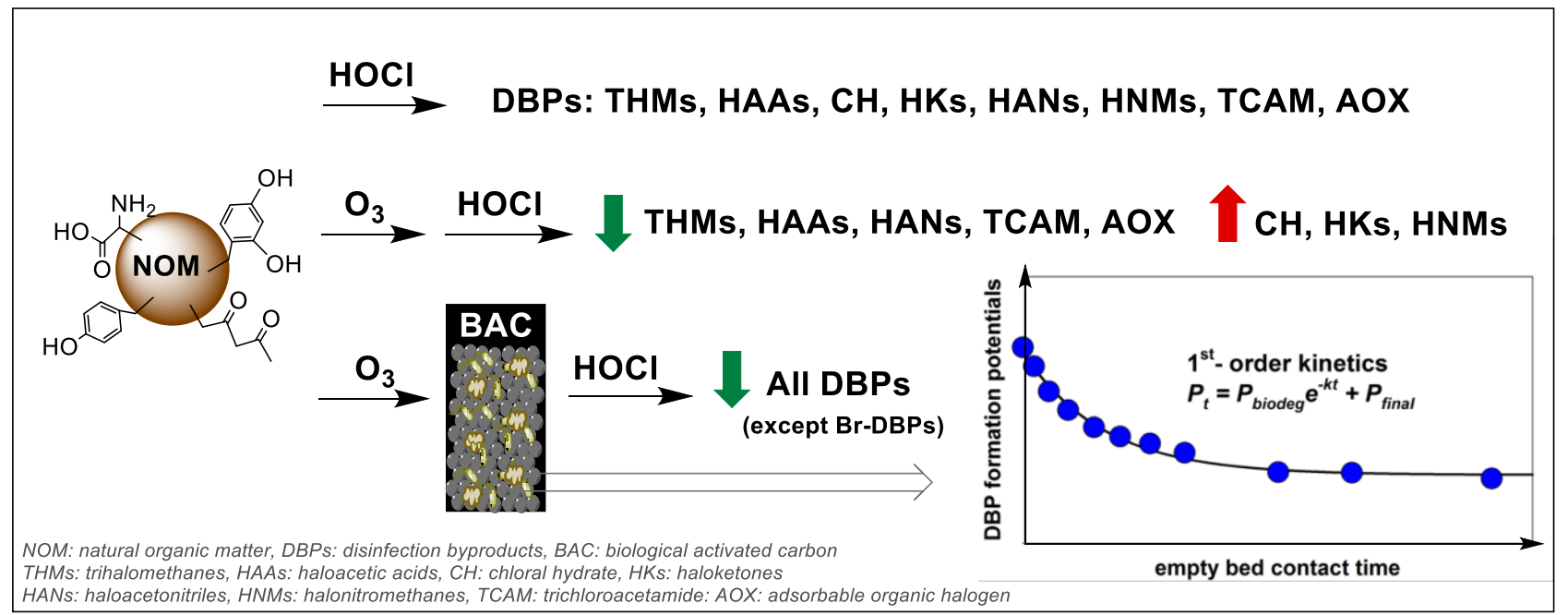

NOM: natural organic matter, DBPs: disinfection byproducts, BAC: biological activated carbon
THMs: trihalomethanes, HAAs: haloacetic acids, CH: chloral hydrate, HKs: haloketones
HANs: haloacetonitriles, HNMs: halonitromethanes, TCAM: trichloroacetamide: AOX: adsorbable organic halogen

ACCEPTED MANUSCRIPT

Biodegradability of DBP precursors after drinking water ozonation

Glen Andrew De Vera[1], Jurg Keller[1], Wolfgang Gernjak[1,2,3], Howard Weinberg[4], Maria José Farré[1,2,*]

[1]The University of Queensland, Advanced Water Management Centre, Queensland 4072, Australia

[2]ICRA, Catalan Institute for Water Research, Scientific and Technological Park of the University of Girona, H_2O Building, Emili Grahit 101, 17003 Girona, Spain

[3]ICREA, Catalan Institute for Research and Advanced Studies, 08010 Barcelona, Spain

[4]University of North Carolina at Chapel Hill, Department of Environmental Sciences and Engineering, 146A Rosenau Hall, Chapel Hill, North Carolina 27599, United States

[*]Corresponding author: Maria José Farré: phone: (+34) 972 18 33 80, email: mjfarre@icra.cat

Submitted to Water Research

ACCEPTED MANUSCRIPT

Abstract

Ozonation is known to generate biodegradable organic matter, which is typically reduced by biological filtration to avoid bacterial regrowth in distribution systems. Post-chlorination generates halogenated disinfection byproducts (DBPs) but little is known about the biodegradability of their precursors. This study determined the effect of ozonation and biofiltration conditions, specifically ozone exposure and empty bed contact time (EBCT), on the control of DBP formation potentials in drinking water. Ozone exposure was varied through addition of H_2O_2 during ozonation at 1 mgO_3/mgDOC followed by biological filtration using either activated carbon (BAC) or anthracite. Ozonation led to a 10% decrease in dissolved organic carbon (DOC), without further improvement from H_2O_2 addition. Raising H_2O_2 concentrations from 0 to 2 mmol/mmolO_3 resulted in increased DBP formation potentials during post-chlorination of the ozonated water (target Cl_2 residual after 24 h = 1 – 2 mg/L) as follows: 4 trihalomethanes (THM4, 37%), 8 haloacetic acids (HAA8, 44%), chloral hydrate (CH, 107%), 2 haloketones (HK2, 97%), 4 haloacetonitriles (HAN4, 33%), trichloroacetamide (TCAM, 43%), and adsorbable organic halogen (AOX, 27%), but a decrease in the concentrations of 2 trihalonitromethanes (THNM2, 43%). Coupling ozonation with biofiltration prior to chlorination effectively lowered the formation potentials of all DBPs including CH, HK2, and THNM2, all of which increased after ozonation. The dynamics of DBP formation potentials during BAC filtration at different EBCTs followed first-order reaction kinetics. Minimum steady-state concentrations were attained at an EBCT of about 10 – 20 min, depending on the DBP species. The rate of reduction in DBP formation potentials varied among individual species before reaching their minimum concentrations. CH, HK2, and THNM2 had the highest rate constants of between 0.5 and 0.6 min^{-1} followed by HAN4 (0.4 min^{-1}), THM4 (0.3 min^{-1}), HAA8 (0.2 min^{-1}), and AOX (0.1 min^{-1}). At an EBCT of 15 min, the reduction in formation potential for most DBPs was less than 50% but was higher than 70% for CH, HK2, and THNM2. The formation of bromine-containing DBPs increased with increasing EBCT, most likely due to an increase in Br^-/DOC ratio.

ACCEPTED MANUSCRIPT

Overall, this study demonstrated that the combination of ozonation and biofiltration is an effective approach to mitigate DBP formation during drinking water treatment.

Keywords: *biofiltration, disinfection byproducts, empty bed contact time, ozonation*

ACCEPTED MANUSCRIPT

1. Introduction

Ozonation has been widely used as an intermediate process to reduce disinfection byproduct (DBP) formation associated with drinking water chlorination (Hua and Reckhow 2013, Sedlak and von Gunten 2011). Ozonation can significantly alter the structure and reactivity of natural organic matter (NOM) (Wenk et al. 2013) resulting in the formation of a mixture of compounds with lower molecular weight and aromaticity, and higher carboxylic acid functionality (Carlson and Amy 1998, Urfer et al. 1997). This oxidative treatment increases the assimilable organic carbon (AOC) content (Hammes et al. 2006, Ramseier et al. 2011) which is of great concern for water utilities because of increased bacterial regrowth potential in distribution systems. On the other hand, biofiltration can take advantage of this process as a means of removing additional DBP precursors from the water prior to final disinfection, while at the same time reducing AOC.

Several studies have shown that biofiltration can remove some DBP precursors and the associated chlorine demand as well as biodegradable organic carbon which includes products formed by ozonation in water such as aldehydes and carboxylic acids, among others (Chu et al. 2012, Gagnon et al. 1997, Krasner 2009, Speitel et al. 1993, Weinberg et al. 1993). This can be achieved because of the presence of biofilm (i.e., heterotrophic bacteria attached to a media) that utilizes biodegradable NOM as a carbon source for energy production (Urfer et al. 1997). The degree of NOM removal is affected by the characteristics of both the influent ozonated water and the biofilter. The ozonated water quality varies depending on whether ozonation conditions promote O_3 over hydroxyl radical ($^{\bullet}OH$) reactions or vice versa. However, information about the effects of these conditions on biofiltration is currently missing in the literature. Moreover, filter media, biomass, and operational parameters such as empty bed contact time (EBCT) can impact the biofilter performance. For example, Melin and Odegaard (2000) evaluated the removal rate of influent ozonation byproducts aldehydes and aldo- and keto-acids as a function of EBCT. Several modelling studies attempted to gain a mechanistic understanding of the biodegradation kinetics of

NOM (Gagnon and Huck 2001, Huck and Sozanski 2008). Huck et al. (1994) reported a linear relationship between the removal rate and filter influent concentrations (i.e., a first-order process) of the following: biodegradable and assimilable organic carbon, chlorine demand, and precursors of trihalomethanes (THMs) and adsorbable organic halogen (AOX). There are, however, no published kinetic studies in the literature describing the impact of combined ozone/biofiltration on the formation potentials of chloral hydrate (CH), haloketones (HKs) and the more toxic nitrogen-containing DBPs (Plewa et al. 2008) such as halonitromethanes (HNM) which are the organic DBPs most commonly elevated when treating ozonated waters with chlorine. If a first-order kinetics would hold true for these DBPs as well, water utilities might be able to predict and set biofiltration conditions that could control DBP formation during drinking water treatment.

This study, therefore, evaluated (1) the effect of O_3 and $^{\bullet}OH$ reactions on the biodegradability of ozonated waters and (2) the reduction in formation potentials of different families of DBPs including THMs, haloacetic acids (HAAs), CH, HKs, haloacetonitriles (HANs), HNMs, and trichloroacetamide (TCAM) by ozone-biofiltration treatment with varying EBCT. These objectives were achieved by conducting ozone dosing experiments followed by batch biodegradation and once-through column experiments using anthracite and biological activated carbon (BAC) as media and subsequent chlorination. As little is known about biodegradation of DBP precursors and most biofiltration studies have only focused on removal of biodegradable organic carbon and ozonation by-products, this study provides important novel insights on the impact of ozonation and biofiltration on DBP precursors and subsequent byproduct formation in chlorinated drinking water.

ACCEPTED MANUSCRIPT

2. Materials and methods

2.1. Water sample and bioactive media

The water and bioactive media used in this study were obtained from drinking water treatment plants in Southeast Queensland, Australia (SEQ). Two types of bioactive media were used: (i) anthracite (AN) with an effective size of 1.2-1.3 mm and apparent density of 650 kg/m^3 taken from the top layer of a primary filter (i.e., after pre-ozonation, coagulation, and sedimentation) which had been used for more than 5 years and (ii) granular biological activated carbon (BAC) with an effective size of 0.7-0.9 mm and apparent density of 435 kg/m^3 (ACTICARB GA1000N, Activated Carbon Technologies Pty Ltd, Australia) taken from the top layer of the post-O_3 filter that had been in operation for more than two years. Adsorption would not, therefore, be expected to play a major role on NOM removal in either of these media. As described in Text S1, the bioactive media were from the advanced water treatment plant depicted in Fig. S1 (Supplementary Material).

2.2. Batch ozonation

Ozone stock solutions were prepared fresh daily in MilliQ water by sparging gaseous ozone generated from pure oxygen (99.995%; Coregas, Australia) using an Anseros COM-AD-04 ozone generator (Anseros, Germany). Concentrations of the stock solutions were determined spectrophotometrically using the absorbance at 258 nm (ε=3000 M^{-1}cm^{-1}) (Elovitz and von Gunten 1999). Appropriate volumes of the ozone stock solution were spiked into water samples (pH = 7) to obtain the desired transferred ozone dose, assuming 100% transfer efficiency. Ozone was allowed to fully decay prior to biological treatment.

2.3. Experiments carried out

Three sets of experiments were performed to investigate the biodegradability of DBP precursors at different ozonation and biodegradation conditions. The first set involved water samples treated with different O_3 doses and subsequently exposed to bioactive anthracite. Bioactivity in these batch tests was confirmed by measuring consumption of biodegradable organic carbon. A control

experiment with 0.3 mM sodium acetate (DOC = 7.2 mg/L; >99%, Ajax Finechem, Australia) showed an 84% DOC removal after 8 days of exposure with the bioactive anthracite (Fig. S2a). The second set involved column experiments using BAC and bioactive anthracite media fed with water ozonated with and without H_2O_2. These two sets of experiments evaluated optimization of the ozonation process for better NOM biodegradability. The third set of experiments focused on studying biofiltration performance by varying the EBCT of the BAC columns. For these column experiments, bioactivity was confirmed by constantly monitoring dissolved oxygen (DO) consumption by the bioactive media and removal of influent DOC. Similar to other studies (Evans et al. 2013, Liao et al. 2016, Persson et al. 2007, Pipe-Martin 2008, Rattier et al. 2014), DO measurements served as the indicator of oxygen consumed by microorganisms during respiration and an indirect proof of aerobic biological activity in the filters.

2.3.1. Batch biodegradation and column filtration

Prior to biodegradation, ozonation experiments (pH 7) were performed on the water sample by adding ozone to create ozone to DOC ratios (mg/mg) ranging from 0.4 to 1. These samples were not buffered since preliminary results revealed that 1 mM phosphate ($NaH_2PO_4 \cdot 2H_2O$, >99%, Ajax Finechem, Australia and $Na_2HPO_4 \cdot 2H_2O$, ≥99.5%, Merck, Germany) and 4-9 mM $NaHCO_3$ (>99.5%, Sigma-Aldrich, USA) inhibited biodegradation of NOM (Fig. S2a and S2b). Instead, the pH of the ozonated aqueous samples was readjusted to pH 7 using small quantities of 0.5 M HCl (Merck, Germany) prior to contact with the bioactive anthracite in order to mimic the actual influent pH during biofiltration in a full-scale plant. 500 mL of ozonated water sample was mixed with 170 g of bioactive anthracite with contact time of 7 days at ambient temperature.

Column experiments (Fig. S3) were also performed using bioactive anthracite and BAC. Filtration was carried out upflow to avoid bed compaction, clogging, and to obtain a more uniform distribution of organic matter through the filter media. The biofiltration system was comprised of 4 glass columns (two each for columns for non-ozonated and ozonated feed lines; internal diameter: 1

cm; length: 12 cm; manufactured at University of Queensland Glassblowing Services) containing the bioactive media (bed volume = 6.5 mL), a multi-channel peristaltic pump (Sci-Q 323, Watson Marlow, USA), a dissolved oxygen (DO) probe (WTW, Germany), ozonated water as feed, and effluent collection bottles. The ozone dose employed for these experiments was 1.2 mgO_3/mgDOC. Each biofiltration line was connected to the columns using Norprene tubing (Cole-Palmer, USA). Biofiltration experiments were performed at room temperature (22 ± 1^0C), influent water DO of 9.0 ± 0.8 mg/L and an EBCT of 11 minutes. To condition the media and equilibrate influent concentrations through the filter, 100 bed volumes of the ozonated water sample were pumped at a rate of 0.6 mL/min prior to sampling. The effluent for this conditioning step was discarded.

2.3.2. Biofiltration of samples treated with O_3/H_2O_2

Ozone decomposition was varied by adding increasing H_2O_2 concentrations. Ozonation was conducted at a dose of 1 mgO_3/mgDOC with H_2O_2 concentrations ranging from 0 to 2 mmol H_2O_2/mmol O_3. Stock solutions of H_2O_2 (30%, Merck, Germany) were previously standardized spectrophotometrically at 240 nm (ε = 40 $M^{-1}cm^{-1}$) (Bader et al. 1988) while the H_2O_2 concentration in samples was determined using the method described by Nogueira et al. (2005). Prior to DBP formation potential tests and/or biofiltration, H_2O_2 was quenched by adding 1.4 g of MnO_2 (≥ 99%, Sigma-Aldrich, Australia) to 1 L ozonated sample (Sarathy 2004). MnO_2 was chosen as an adequate H_2O_2 quencher since it has been reported to not affect bacterial growth. For example, MnO_2 quenching of H_2O_2 did not interfere with AOC measurements, unlike other common quenchers such as catalase and sodium thiosulfate (Sarathy 2004). Fig. S4 illustrates the removal of H_2O_2 after addition of MnO_2. Bioactive anthracite and BAC were used separately as biofiltration media each with a 7 mL bed volume and 11 min EBCT.

2.3.3. Biofiltration at different EBCT values

Each biofiltration line was connected to two BAC columns with a total bed volume of 12 mL. Three parallel lines were used for replicate measurements. Although the biomass concentration in

the biofilters was not measured, bioactivity was confirmed through measurements of DO consumption and NO_3^- evolution (Fig. S5) due to the presence of nitrifiers as observed in a preliminary study. Effluent collection was performed at the lowest flow rate first (0.22 mL/min) and increased successively to the highest flow rate (4.0 mL/min) which corresponds to filtration at decreasing EBCT (ratio of bed volume to influent flow rate). Samples were collected before biological filtration and at the following EBCTs: 3, 5, 8, 11, 15, 19, 30, 39, and 55 min. In between sampling at the different EBCTs, mild backwashing was done using a sample-containing syringe connected online. After this step, at least 3 bed volumes of the ozonated sample were pumped through the columns and discarded. This volume was assumed sufficient to flush the sample used in a previous condition out of the columns.

Biofiltered samples (250 mL) were collected in acid-washed amber-colored glass bottles and stored at 4 ^{0}C prior to subsequent analyses. Sample collection during column experiments was performed within a week to avoid possible changes in biomass and biofilm characteristics that may be a significant variable on NOM removal. A constant biological activity in the media was desired to be able to compare the reactivity of different precursors with changes in EBCT.

2.4. DBP formation potential tests

DBP formation potential tests were as described in previous studies (De Vera et al. 2015, Doederer et al. 2014, Farré et al. 2013). Briefly, sodium hypochlorite (reagent grade, available chlorine 4 − 4.99%, Sigma-Aldrich, USA) was added to samples buffered at pH 7 with 10 mM phosphate. For every experiment, the concentration of sodium hypochlorite added was based on prior chlorine demand tests with the same water and aimed to have a residual of 1 – 2 mg/L as Cl_2 after a 24 h reaction. Chlorine residual in samples was measured using the *N*,*N*-diethyl-*p*-phenylenediamine free chlorine colorimetric method (Hach, USA). After one day of contact time, residual chlorine was quenched with either L-ascorbic acid (≥99%, Sigma-Aldrich, China), ammonium chloride (99.5%, Sigma-Aldrich, Japan), or sodium sulfite (≥98%, Sigma-Aldrich,

Japan) depending on the subsequent extractions for neutral-extractable DBPs, HAAs, or AOX, respectively.

2.5. Analytical methods

2.5.1. Dissolved oxygen and inorganic nitrogen

Influent and effluent DO concentrations were measured on-line in a gas tight flow through cell using a WTW Multi 3420 meter equipped with DO probe FDO 925 (DO measuring range specified by manufacturer = 0 – 20 mg/L, WTW, Germany). Ammonia, nitrite and total NO_x (i.e., sum of NO_2^- and NO_3^-) were measured on samples collected before and after biofiltration by a Lachat QuikChem8500 Flow Injection Analyzer (Hach Company, USA) using Lachat methods 31-107-06-1-B (NH_4^+), 31-107-04-1-A (NO_x), and 31-107-05-1-A (NO_2^-). The method reporting limits (MRL; 3 × method detection limit (MDL) (NATA 2013); MDL = standard deviation of at least 7 replicate analyses of the lowest laboratory standard in reagent blank × Student's t-statistic for a 99% confidence level and n-1 degrees of freedom (USEPA 2010)) were 4 µg/L for NH_4^+-N (measuring range = 4 – 900 µg/L), 0.6 µg/L for NO_2^--N (measuring range = 0.6 – 72 µg/L), and 4 µg/L for NO_x-N (measuring range = 4 – 900 µg/L).

2.5.2. Dissolved organic carbon and UV absorbance

The DOC of 1.2 µm GF/C filtered samples was measured with a Shimadzu TOC-L analyzer that was also equipped with a TNM-L total nitrogen analyzer unit and ASI-L autosampler (Shimadzu, Japan). The MRL for DOC was 0.3 mg/L (measuring range = 0.3 to 25 mg/L). UV absorbance at 254 nm (UV_{254}) was measured with a Varian Cary 50 Bio UV-Visible spectrophotometer (Varian, Australia).

2.5.3. Size exclusion chromatography (SEC)

The molecular weight distribution of NOM in each water sample (untreated, ozonated, and biofiltered) was evaluated using a Shimadzu prominence LC-20AT high performance liquid chromatograph (HPLC, Shimadzu, Japan) equipped with a SIL-20A HT autosampler and a

Toyopearl HW-50S SEC column (250 mm x 20 mm packing material; Tosoh, Japan). The unit was connected to a SPD-M20A diode array detector (UVD) and a GE Sievers 900 portable online total organic carbon analyzer (OCD) with an inorganic carbon remover (GE, USA). The retention times of eluted volumes were calibrated against polyethylene glycol standards (Agilent, UK) in order to convert to molecular weight. The analyses used a 25 mM phosphate mobile phase (pH 6.85), 1 mL/min flow rate, 1100 μL injection volume, 35 ^{0}C oven temperature, and 100 min analysis time.

2.5.4. Volatile neutral extractable DBPs

The following volatile DBPs were analyzed in aqueous samples at pH 7 after duplicate extractions with methyl tert-butyl ether (MtBE; 99.9%, Sigma-Aldrich, USA): (a) four trihalomethanes (THM4: trichloromethane (TCM), dibromochloromethane (DBCM), bromodichloromethane (BDCM), tribromomethane (TBM)), four haloacetonitriles (HAN4: trichloroacetonitrile (TCAN), dichloroacetonitrile (DCAN), bromochloroacetonitrile (BCAN), dibromoacetonitrile (DBAN)), two haloketones (HK2: 1,1-dichloropropanone (DCP), 1,1,1-trichloropropanone (TCP)), two trihalonitromethanes (THNM2: trichloronitromethane (TCNM), tribromonitromethane (TBNM)), chloral hydrate (CH), and trichloroacetamide (TCAM). Iodinated DBPs (e.g., dichloroiodomethane, bromochloroiodomethane, dibromoiodomethane, chlorodiiodomethane, bromodiiodomethane, triiodomethane, chloroiodoacetamide, bromoiodoacetamide, and diiodoacetamide), and most other haloacetamides (e.g., dichloroacetamide, bromochloroacetamide, dibromoacetamide, bromodichloroacetamide, dibromochloroacetamide, and tribromoacetamide) were also measured but not detected in samples chlorinated after ozonation. Text S2 and Table S1 provide more details on the DBPs and standards used. MtBE extracts containing the volatile DBPs and the internal standard (1,2-dibromopropane) were injected into an Agilent 7890A gas chromatograph equipped with two independent electron-capture detector (GC/ECD) (Agilent, China) connected to a separate DB-5 and a DB-1 Agilent column (30 m length x 0.25 mm inner diameter x 1.0 um film thickness each) and two injectors.

Pulsed splitless injection was used at 140 ^{0}C. The oven temperature program started at 35 ^{0}C for 25 min, followed by three ramps to have a total analysis time of 81 min: (1) 100 ^{0}C at 2 ^{0}C/min (2 min holding time), (2) 200 ^{0}C at 5 ^{0}C/min, and (3) 280 ^{0}C at 50 ^{0}C/min. The ECD temperature was set at 300 ^{0}C. The MRL for all volatile DBPs was 0.1 µg/L (measuring range = 0.1 – 200 µg/L) with recoveries normally ranging from 80% to 120%.

2.5.5. Adsorbable organic halogen (AOX)

The analysis of AOX was based on previously reported methodologies (De Vera et al. 2015, Farré et al. 2013, Stalter et al. 2016, Yeh et al. 2014). In this method, 10 mL of quenched aqueous sample was first acidified with 10 µL of concentrated HNO_3 (70%, Sigma-Aldrich, Australia). The acidified sample was then passed through two consecutive activated carbon cartridges (50 mg C in 3 mm ID Euroglass, CPI International, USA) using a 10 mL gas-tight Hamilton syringe. The cartridges were washed with 8.2 g/L potassium nitrate (≥99%, Sigma-Aldrich, Australia) at a rate of about 5 mL/min to remove inorganic halides. The activated carbon was next transferred to sample boats for pyrolysis at 1000 ^{0}C (in the presence of oxygen) using a Mitsubishi AQF-2100 Automated Quick Furnace unit connected to a Dionex ICS-2100 Dual Channel Ion Chromatograph (IC) system (Thermo Fisher Scientific, Australia). Using argon as a carrier gas, the halogens produced from pyrolysis were then reduced to halide ions in a 10 mL absorption solution (0.003% H_2O_2 with 1 mg/L phosphate). Chloride, bromide, and iodide ions were then quantified by IC with MRLs of 12, 6, and 15 µg/L, respectively. The commonly used linear range was up to 800 µg/L for bromide, 2000 µg/L for chloride, and 400 µg/L for iodide. AOX is reported as a Cl equivalent concentration (µM as Cl), which refers to the sum of the equivalent concentrations of adsorbable organic chlorine, bromine, and iodine multiplied by the atomic mass of Cl.

2.5.6. *Haloacetic acids (HAAs)*

Eight haloacetic acids (trichloroloacetic acid (TCAA), bromodichloroacetic acid (BDCAA), chlorodibromoacetic acid (CDBAA), dichloroacetic acid (DCAA), bromochloroacetic acid

(BCAA), dibromoacetic acid (DBAA), monochloroacetic acid (MCAA), and monobromoacetic acid (MBAA)) were measured at Queensland Health Forensic and Scientific Services (QHFSS) using an acidic, salted microextraction followed by derivatization with acidic methanol and GC/ECD analysis (US EPA Method 552.3 (Domino et al. 2003)). Tribromoacetic acid was not analyzed due to its low stability. The MRL for all HAA species was 5 μg/L.

2.5.7. *Bromide and bromate*

Bromide and bromate were measured at QHFSS with a Metrohm 861 Advanced Compact Ion Chromatograph (Metrohm, Switzerland) equipped with a CO_2 suppressor, a Thermo AS23 column, Thermo AG23 guard column and a 50 μL sample loop. The eluent was a carbonate (4.5 mM Na_2CO_3)/bicarbonate (0.8 mM $NaHCO_3$) mixture with a 1 mL/min flow rate. The MRLs for bromide and bromate of QHFSS were 5 and 10 μg/L, respectively.

ACCEPTED MANUSCRIPT

3. Results and Discussions

3.1. *Effect of ozonation and biodegradation on formation potentials of halogenated DBPs produced by subsequent chlorination*

3.1.1. Ozonation

Ozone is known to significantly alter NOM characteristics because of its reaction towards their electron-rich moieties which include activated aromatic systems, olefins, and non-protonated amines. These reactions favor the effectiveness of biofiltration if it follows ozone treatment and impact DBP formation by post-chlorination. The reactions of ozone with such moieties have been extensively studied in the literature (von Gunten 2003, von Sonntag and von Gunten 2012). Briefly, ozone reacts with phenolic compounds (Fig. 1a) via an ozone adduct which proceeds primarily to ring cleavage, formation of muconic-type compounds, and eventually resulting in aliphatic aldehydes and ketones (Hammes et al. 2006, Ramseier and von Gunten 2009). In our study, ozonation of the water sample (1 mgO_3/mgDOC) caused an 11% decrease in DOC and a 56% decrease in SUVA (Fig. S6). These results were consistent with the typical degree of mineralization of NOM (~10% at 1 mgO_3/mgDOC) (Nothe et al. 2009) resulting from decarboxylation reactions that occur during further oxidation of substantially oxidized NOM (von Sonntag and von Gunten 2012). The high decrease in SUVA supports the likelihood that the ring-opening mechanism shown in Fig. 1a for phenolic compounds occurred in our reactions. These observations were in agreement with the SEC images that show significant removal of NOM (humics and building block region) by ozone with the UV_{254} detector (Fig. S7a) but barely any with the organic carbon detector (Fig. S7b; OCD). The results indicate that certain UV absorbing units of NOM were partially oxidized and transformed to lower molecular weight compounds rather than being mineralized since the overall DOC was mostly unchanged. Minor pathways could generate products such as catechol, hydroquinone, and quinones (Ramseier and von Gunten 2009) especially at lower O_3 doses (Chon et al. 2015). For olefins (Fig. 1b), the ozone reaction occurs via a Criegee mechanism that involves

318 cleavage of the C=C double bond and formation of carbonyl compounds (Criegee 1975). For
319 amines (Fig. 1c), an ozone adduct on the nitrogen atom leads to formation of *N*-oxide for tertiary
320 amines and hydroxylamine for primary and secondary amines (von Gunten 2003). A recent study
321 also reported formation of nitromethane from ozonation of methylamine (McCurry et al. 2016).
322 Amine radical cations can also be formed leading to dealkylated amines and ketones or aldehydes
323 (von Sonntag and von Gunten 2012). These ozonation transformation products could be formed
324 along with products from $^{\bullet}OH$ reactions since ozonation conditions at treatment plants do not
325 scavenge for these radicals. Addition reactions are very common for $^{\bullet}OH$ since the radicals readily
326 add to C-C and C-N bonds (von Sonntag and von Gunten 2012).

327 These transformation products can affect the subsequent DBP formation potentials during post-
328 chlorination, as shown in this study. Consistent trends were observed for all the DBPs presented in
329 Figs. 2-5. Results are presented as relative residual concentrations (C/C_0) to show the extent of the
330 change in concentrations with respect to C_0 or the concentration resulting from chlorination alone
331 (i.e., without prior ozonation and biodegradation). Analyte concentrations are summarized in Tables
332 S2-S6.

333 The mechanisms of Figs. 1a and 1b show example precursors for aliphatic aldehydes and
334 ketones formed from ozone. In this study CH and HK2 were found to more than double in
335 concentration at 1 $mgO_3/mgDOC$ that could have resulted from ring-opening of phenolic groups in
336 NOM (see decrease in SUVA in Fig. S6). THM4 and HAA8 decreased by about 30% and 10%,
337 respectively, after ozonation at the same O_3 dose (Table S6) because reaction sites for chlorine such
338 as those in activated aromatic systems, β-diketones and β-diketoacids will have already been
339 oxidized by O_3. HAN4 and TCAM (Table S2, 1 $mgO_3/mgDOC$) also decreased in concentration
340 (HAN4 = 0.13 to 0.11 µM; TCAM = 0.014 to 0.006 µM) most likely because of the oxidation of the
341 precursor amino groups (Fig. 1c), leading to pronounced formation of THNM2 especially with
342 increasing O_3 dose (0.007 to 0.068 µM). Lower AOX (19.7 to 15.7 µM Cl^-, Table S3) was also

observed which suggests the benefit of ozonation in decreasing formation potentials of other non-volatile DBPs that were not measured. After O_3/HOCl treatment, bromine-containing DBPs namely tribromomethane (TBM), dibromochloromethane (DBCM), dibromoacetic acid (DBAA), dibromoacetonitrile (DBAN), and tribromonitromethane (TBNM) also increased (Tables S2 and S3) because of the production of more hydrophilic NOM during ozonation which are more amenable to HOBr than HOCl reactions (Hua and Reckhow 2013, Westerhoff et al. 2004). HOBr, produced from oxidation of bromide during chlorination and ozonation, can react with NOM to form the previously mentioned bromo-organic DBPs (Gruchlik et al. 2014). Under the conditions used, no bromate was observed above the MRL (10 μg/L) probably because of the high reactivity of NOM that competes with bromide in reactions with O_3 and $^{\bullet}OH$.

3.1.2. Biodegradation

The impact of ozonation on biodegradability of the water samples was evaluated using (1) batch experiments with bioactive anthracite and (2) biofiltration columns containing either anthracite or BAC. The results of batch biodegradation experiments using bioactive anthracite (contact time = 7 days) are shown in Fig. 2 while biofiltration experiments (EBCT = 11 min) are shown in Fig. 3.

3.1.2.1. Biodegradation before ozonation

Biodegradation experiments without pre-ozonation ("No O_3" in Figs. 2 and 3) yielded notably different results for anthracite batch and column filtration experiments, likely due to differences in contact time (i.e., 7 day exposure with anthracite for batch biodegradation and 11 min for column experiment). This longer contact time may explain the higher DOC removals (38%) and better reduction of formation potentials of THM4 (51%), CH (52%), and HK2 (76%) in Figs. 2b – 2d (batch biodegradation) compared to their equivalents using the biofilter columns (Figs. 3a – 3d; % removal: DOC = 12%, THM4 = 30%, CH = 34%, HK2 = 32%). After batch biodegradation, higher HAN4 formation potentials were observed which could have been caused by release of soluble

368 microbial products (SMPs) (e.g., nucleic acids, proteins, amino acids) (Rittman et al. 1987) during
369 long contact times. THNM2 precursors (Figs. 2f and 3f), which were present at very low
370 concentrations (~0.01 µM) before ozonation, had low removals of less than 6% which suggests that
371 non-ozonated THNM precursors were not readily biodegradable. This result was in agreement with
372 the observations by Wadhawan et al. (2014) who demonstrated the importance of ozonation in
373 increasing the concentrations of biodegradable DON. Biofiltration of non-ozonated samples did not
374 change the resultant TCAM levels (Fig. 3g) whereas at the longer contact times in batch
375 biodegradation tests (Fig. 2g), removals of 50% were achieved indicating the presence of TCAM
376 precursors that may biodegrade slowly. The relatively high error bars for TCAM are a result of its
377 concentrations near the MRL. Because of the contrasting effects of TCAM and HAN4 in Figs. 2e
378 and 2g, it is likely that TCAM precursors are independent from HAN4 precursors in the
379 biodegraded water sample. The SMP released during batch biodegradation could be a major
380 contributor to HAN4 formation, while TCAM could predominantly come from humic substances of
381 the water sample (Huang et al. 2012). For AOX, biofiltration of non-ozonated precursors only
382 resulted in a 2 – 13% decrease in formation potentials.

383 *3.1.2.2. Biodegradation after ozonation*

384 Combining ozonation (1 mgO_3/mgDOC) with batch anthracite biodegradation resulted in an
385 overall reduction of 54% of DOC (Fig. 2a, Table S2: No O_3 = 9.8 mg/L DOC; No O_3 + AN = 6.0
386 mg/L DOC; O_3 only = 8.7 mg/L DOC; combined O_3 + AN = 4.5 mg/L DOC). The observed better
387 DOC removal (O_3 + AN versus O_3 only) is most likely due to the formation of smaller, more
388 hydrophilic, and readily biodegradable compounds following ozonation such as aldehydes, ketones,
389 and carboxylic acids (Fig. 1) (Hammes et al. 2006, Weinberg et al. 1993). For aromatic compounds,
390 ring cleavage products have been estimated to be more biodegradable compared to their parent
391 compounds (Hubner et al. 2015). These products are reported to be biodegraded via a pathway that
392 leads to carboxylate as shown in the University of Minnesota biocatalysis/biodegradation database

(Gao et al. 2010) (refer to Table S7 for a list of different biotransformation (bt) rules relevant to this study). No significant change in biodegradability was associated for possible aromatic hydroxylation products such as catechols (Hubner et al. 2015). These observations support the increase in SUVA after biodegradation (Fig. S6) since compounds with low UV absorbance are consumed, decreasing the DOC and leaving behind other UV absorbing aromatic compounds (Fig. S7b). The improved biodegradability of NOM also translated to a decrease in THM4, CH, and HK2 formation during post chlorination (shown in Figs. 2b, 2c, and 2d respectively) with the most notable effects on CH and HK2 because of the readily biodegradable aldehyde and ketone precursors.

Aerobic biodegradation of amine compounds is expected to form aldehydes and ketones through oxidative removal of an alkyl substituent from an amine using dehydrogenase enzymes (Gao et al. 2010). In this biodegradation pathway (biotransformation rule bt0063 of the biodegradation database shown in Table S7), aldehydes and ketones are produced if the leaving substituent is attached to a primary or secondary carbon, respectively. Other N-DBP precursors, formed by ozone, containing *N*-oxide, hydroxylamine, and nitromethane moieties can also be biodegraded accordingly (biotransformation rules bt0408, bt0035, bt0086). These transformations resulted in decreased HAN4, THNM2, and TCAM concentrations as shown in Figs. 2e, 2f, and 2g, respectively. Precursors of THNM2 were observed to be very biodegradable with a decrease in formation potentials of up to 98%. This decrease was mostly caused by the removal of trichloronitromethane precursors. Although formed at low concentrations, tribromonitromethane was found to increase because of higher bromine substitution with subsequent chlorination of biodegraded water samples. This was also observed for other brominated THMs and HANs confirming the known influence of the bromide to carbon ratio in DBP speciation (Fig. S8). Since bromide was not consumed as DOC decreased during biodegradation, the bromide to carbon ratio increased leading to the formation of more available HOBr in relation to the reduced NOM

concentration. Due to the higher electrophilicity of HOBr compared to HOCl (Heeb et al. 2014, Symons et al. 1993, Westerhoff et al. 2004), halogenation by HOBr is favored resulting in formation of more brominated DBPs. The apparent rate constants of bromine reactions (pH 7) were reported to be up to 3 orders of magnitude higher than those of chlorine reactions (Heeb et al. 2014). In addition, better bromine substitution occurs especially for ozonated waters since hydrophilic organic materials (e.g., aliphatic products of ozone) were found to be more reactive to HOBr compared to hydrophobic fractions (Hua and Reckhow 2007a, Liang and Singer 2003).

To simulate conditions commonly encountered in actual water treatment conditions, the results of the batch biodegradation experiments were confirmed using bench-scale columns with anthracite and BAC (Fig. 3, Table S3). The extent of DOC removal using both biofilters was similar (33-34 %) after an EBCT of 11 min. The results of SEC with either a UV or organic carbon detector (Fig. S7) showed that this DOC decrease was a result of removal of low molecular weight compounds (*ca.* 10^3 g/mol) consistent with their transport across cell membranes and attack by metabolic enzymes during biodegradation (Nishijima and Speitel 2004). Similar trends were observed for the DBP formation potentials suggesting that comparable enzymatic functions were responsible for biodegradation in both media. All DBPs, including those that increased after ozonation (e.g., CH, HK2, and THNM2), decreased compared to their initial DBP formation potential after biofiltration. For AOX, a reduction of about 45% compared to non-ozonated and non-biofiltered conditions was observed for samples treated with combined ozonation and biofiltration (Fig. 3h).

3.2. Process optimization

3.2.1. Ozonation: Use of O_3/H_2O_2 before biofiltration

Since DBP formation potentials can be affected differently by ozone and $^{\bullet}$OH reactions (De Vera et al. 2015), the effect of ozone exposure on the biodegradability of DBP precursors was investigated. This was achieved through batch experiments involving ozone with and without addition of H_2O_2 to the water samples. Although no $^{\bullet}$OH concentration measurements were made in

443 this study, it has been well-established that the presence of H_2O_2 accelerates O_3 decay through
444 formation of $^{\bullet}OH$ and superoxide radical ($O_2^{\bullet-}$) which further reacts with O_3 (von Gunten 2003, von
445 Sonntag and von Gunten 2012). Thus, at conditions with higher H_2O_2 concentrations, O_3 would
446 decay faster and be transformed more quickly to $^{\bullet}OH$.

447 Fig. 4 shows the changes in DOC resulting from O_3/H_2O_2 and biofiltration treatment and the
448 impact of these treatments on DBPs formed by subsequent chlorination. At all H_2O_2 doses, source
449 DOC decreased by no more than 10% after ozonation, similar to the values obtained in Figs. 2 and
450 3. After biofiltration of the ozonated waters using both anthracite and BAC, a ~30% DOC removal
451 was achieved. The remaining ~6 mg/L DOC (Tables S4 and S5) represents the non-biodegradable
452 fraction of NOM as classified by Yavich et al. (2004). While the DOC remained relatively
453 unchanged at all H_2O_2 concentrations, a different behaviour was observed for DBPs (Figs. 4b – 4i;
454 Tables S4 and S5). Addition of H_2O_2 during ozonation confirmed our previously published work
455 showing that $^{\bullet}OH$ reactions increased the DBP formation potentials of THM4, HAA8, CH, HK2,
456 HAN4, TCAM, and AOX (De Vera et al. 2015). For THNM2, an opposite trend (i.e., lower
457 formation potentials at higher H_2O_2 concentrations) was observed which shows that THNM2
458 precursors are predominantly formed through O_3 reactions (McCurry et al. 2016). When
459 biofiltration was employed after the oxidation process, a dramatic drop in DBP formation potentials
460 was observed in the column effluent especially for CH, HK2, and THNM2 suggesting the high
461 biodegradability of their precursors. The slightly better removal of formation potentials of DBPs
462 with BAC over AN may be attributed possibly to the different surface area and biological activity of
463 each filter media.

464 *3.2.2. Biofiltration: Variation of empty bed contact time (EBCT)*

465 To optimize biofiltration, column experiments using BAC were performed at different EBCTs
466 (3 – 55 min). Bioactivity of the columns was confirmed from the increase in oxygen consumption
467 and nitrate concentration with increasing EBCT (Fig. S5). BAC filtration resulted in about 30%

468 decrease in DOC as shown in Fig. 5a, which is within the range of removal efficiencies reported in
469 the literature (Juhna and Melin 2006). This decrease mostly happened within the first 20 min, with
470 the largest decrease happening within the first three minutes. Such observation supports previous
471 studies (Black and Berube 2014, Carlson and Amy 1998, Yavich et al. 2004) where a characteristic
472 initial period of fast DOC decrease followed by a period of slow decrease was observed. The
473 remaining DOC corresponds to the slowly biodegradable to non-biodegradable DOC. A similar
474 trend was also observed for the formation potentials of all the DBPs studied (Figs. 5b – 5i). These
475 results followed first-order reaction kinetics (Black and Berube 2014, Huck et al. 1994, Melin and
476 Odegaard 2000) and can be modelled using equation (1),

477 $$P_t = P_{biodeg} e^{-kt} + P_f \qquad (1)$$

478 where t is the EBCT (min), k is the specific first-order rate constant (min^{-1}), P_t is the concentration
479 at time t (μM), P_{biodeg} is the biodegradable concentration (μM), and P_f is the minimum contaminant
480 concentration or DBP formation potential (μM) after a certain EBCT. The model fit for DOC and
481 DBP formation potentials was carried out using the software SigmaPlot, version 13.0 (Systat
482 Software, Inc.) and resulted in the kinetic parameters summarized in Table 1. Residuals from the
483 model fit show a normal distribution (P values > 0.05, Shapiro-Wilk test). All measured formation
484 potentials at different EBCTs are presented in Table S6. Further discussion on the first-order
485 dependence of pollutant removal on EBCT is provided in Text S3 and Fig. S9.

486 Following ozonation, THM4 formation potential was reduced by 46% after a BAC EBCT of 15
487 min (i.e., 2.70 μM down to 1.47 μM) and remained at almost the same level up to 55 min. This
488 indicates that THM precursors, mostly for TCM and BDCM, were not completely degraded even at
489 extended EBCTs. In terms of speciation, the decrease in TCM and BDCM was also accompanied
490 by an increase in the more brominated THM species, namely DBCM and TBM. TBM formation
491 potentials increased from 0.003 ± 0.001 to 0.022 ± 0.002 μM in 15 min and continued to increase to
492 0.031 ± 0.001 μM in 55 min, while DBCM started to slightly increase at 15 min (i.e., 0.20 ± 0.02

493 μM to 0.24 ± 0.01 μM in 55 min). These observations can be understood as a result of increased
494 HOBr availability relative to DOC during chlorination since the bromide to DOC ratio increases
495 with increasing EBCT (Fig. S10a). The increase in brominated DBPs (between 0 to 55 min EBCT)
496 was also observed with other DBP groups such as DBAN (0.010 to 0.018 μM), TBNM (0.010 to
497 0.016 μM) and CDBAA (0.028 to 0.050 μM). Hence, an increase in the levels of bromine-
498 containing DBPs with O_3/BAC treatment may occur, especially in source waters containing high
499 bromide concentrations.

500 The concentrations of other non-bromine-containing DBPs such as HK2 and CH were reduced
501 significantly after biofiltration at 10 min EBCT. While their formation potentials increased after
502 O_3/HOCl treatment (i.e., by 73% for HK2 and 111% for CH), their BAC effluent formation
503 potentials of about 0.06 μM for both CH and HK2 appeared to be the lowest attainable during
504 biofiltration. These concentrations were lower than those obtained without ozonation (i.e., HK2 =
505 0.14 μM and CH = 0.17 μM) which confirms the benefit of combined O_3/BAC in reducing
506 formation potentials of these DBPs. The calculated rate constants for these C-DBPs (after
507 ozone/BAC treatment) were 0.50 ± 0.07 min^{-1} for HK2 and 0.58 ± 0.07 min^{-1} for CH, which were
508 highest among the rate constants determined for other DBP groups suggesting the high
509 biodegradability of CH and HK2 precursors.

510 In terms of the HAA species, dihaloacetic acid (DHAA) precursors were removed faster (k =
511 0.18 ± 0.05 min^{-1}) than those of trihaloacetic acids (THAA) (k = 0.06 ± 0.02 min^{-1}) (Fig. S11). At
512 the highest EBCT (55 min) there was a reduction of 58% in DHAA and 47% in THAA in the
513 chlorinated column effluent. The slightly better removal of DHAA than THAA may suggest having
514 more biodegradable precursors (i.e., hydrophilic, low molecular weight) consistent with the findings
515 of Hua and Reckhow (2007a).

516 Similar features to those presented for other DBPs were observed for HAN4, with DCAN being
517 the most dominant HAN produced during chlorination. Low TCAN concentrations were observed

518 due to this compound's low stability (Glezer et al. 1999). Despite HAN4 having the lowest
519 reduction in formation potential (24%, compared to formation potentials after ozonation) after
520 biofiltration at 55 min EBCT, they had a higher k value (0.40 ± 0.14 min^{-1}) than THM4 which had a
521 higher removal (47%) at the same EBCT. This suggests that the biodegradable HAN4 precursors
522 (e.g., aliphatic dissolved organic nitrogen) can be removed faster than their THM4 counterparts.

523 TCNM formation potentials were found to decrease after BAC filtration confirming results
524 from previous studies (Krasner 2009, Lyon et al. 2014). Lowest total concentrations were already
525 achieved at 12 min EBCT and were almost equal to the levels before ozonation. At this EBCT,
526 about 90% of the TCNM formation potential present after ozonation was removed. While good
527 TCNM removals were observed, an increase in TBNM formation potentials became apparent after 5
528 min EBCT. A similar increase in TBNM formation potentials was observed by Lyon et al. (2014) in
529 full-scale plants in SEQ that utilized O_3/BAC. At the highest EBCT tested in the current study,
530 TBNM increased by 52% (Fig. S10b) relative to its formation potential before biofiltration. Despite
531 the contrasting trends of TCNM and TBNM, the sum of their concentrations (THNM2) could still
532 be modelled with a $k = 0.48 \pm 0.01$ min^{-1}, where TBNM accounted for 77% of the remaining P_f.

533 TCAM formation potentials also decreased with first-order kinetics ($k = 0.16 \pm 0.03$ min^{-1})
534 although at a rate that was lower than for HAN4 and THNM2, suggesting differences in
535 biodegradability of their precursors. Based on the calculated rate constant, THNM2 precursors were
536 more readily biodegradable than those of HAN4 and TCAM. This supports the results of Mitch et
537 al. (2009) who showed a higher removal of TCNM compared to DHANs after sequential ozonation,
538 biofiltration, and chlorination. In their study, the median reduction of TCNM formation potentials
539 was 48% while for DHAN it was only 3%.

540 The change in effluent AOX formation potential and chlorine demand followed the trends
541 discussed above. Their first-order reaction kinetics were relatively close (between 0.11 and 0.13
542 min^{-1} (Table 1)). This similarity confirms the intuitive direct relationship of AOX and chlorine

543 demand (slope = 0.17 mg AOX/mg Cl_2 demand, R = 0.99, P=1.2x10^{-9}) as shown in Fig. S12a. AOX
544 formation was also found to correlate well with DOC (Fig. S12a, slope = 0.15 mg AOX/mg DOC,
545 R = 0.98, P=3.7x10^{-7}) which was in agreement with previous studies (Farré et al. 2016). The x-
546 intercept of the AOX versus DOC plot gives a DOC (6.4 mg/L) which is equivalent to 42% of the
547 DOC before ozonation and represents the non-reactive NOM fraction of the water sample.

548 Following biofiltration, AOX in the chlorinated water decreased from 21.7 µM (3 min EBCT)
549 to 12.5 µM (55 min EBCT). At all conditions (i.e., before and after O_3 addition, and after
550 biofiltration from 3 – 55 min EBCTs), the percentage of known and unknown AOX remained
551 relatively constant as depicted in Fig. S13a. Unknown AOX was calculated by subtracting AOX
552 equivalents accounted for by the individually measured DBPs from the measured AOX. In this
553 study, while AOX formation potentials decreased with ozonation and increasing biofiltration
554 EBCTs, the percentage of known AOX remained at 48 ± 4% and the unknown AOX at 52 ± 4 %.
555 These results were comparable to many other studies that reported unknown AOX concentrations of
556 about 50% during chlorination (Reckhow and Singer 1984, Richardson 2003, Singer et al. 1995).
557 As shown in Fig. S13b, the measured AOX in the current study was largely attributed to THM4 (30
558 ± 3%) and HAA8 (13 ± 0.8%) at all applied experimental conditions. These findings are similar to
559 those in a study by Hua and Reckhow (2007b) where they found 25.2% of the total AOX attributed
560 to THMs and 14.4% attributed to HAAs after ozonation (1mgO_3/mgDOC) and subsequent
561 chlorination of a raw water sample. Other DBP groups only had minor contribution. In the current
562 study, THNM2, HAN4, HK2, CH, and TCAM could only explain 0.4%, 0.9%, 1.5%, 2.1%, and
563 0.1%, respectively, of the measured AOX. As the AOX attributed to both THM4 and HAA8
564 remained relatively constant despite differences in the measured AOX concentrations, formation
565 potentials of these two DBP groups were in a linear relationship (i.e., R = 0.98, P <1.5x10^{-4}) with
566 AOX formation potentials (Fig. S12b). In addition to THM4 and HAA8, the AOX values were also
567 strongly correlated with HAN4 (R=0.92, P=6.2x10^{-5}) and TCAM (R=0.98, P=3.7x10^{-7}). The

568 relation of CH and HK2 with AOX was not markedly significant (R=0.65-0.71, P = 0.01 – 0.03)
569 since their formation potentials increased after ozonation. THNM2 had no significant relationship
570 (R=0.21, P = 0.541) with AOX which is also a result of its increase after ozonation. Such
571 correlations might be useful predictors of AOX formation in chlorinated biofilter effluents of water
572 treatment plants.
573

574 **3. Conclusions**

575 Coupling ozonation with biological treatment was found to be beneficial for DBP control. In
576 this study, we investigated the biodegradability of DBP precursors using batch biodegradation
577 experiments with bioactive anthracite and column experiments with bioactive anthracite and BAC.
578 The following conclusions from this study confirm previously published literature:

579 • Ozonation decreased the formation potentials of THM4, HAA8, HAN4, TCAM and
580 increased formation potentials of THNM2, CH, and HK2 with subsequent chlorination.
581 • Compared to conditions that favor $^{\bullet}OH$ reactions (i.e., high H_2O_2 concentrations), direct O_3
582 reactions resulting from the lowest H_2O_2 concentrations led to lower formation potentials of
583 the following DBPs: THM4, HAA8, CH, HK2, HAN4, TCAM, and AOX. The opposite was
584 observed for THNM2.

585 The following novel conclusions can be drawn from this study:

586 • For the water sample tested, the increase in formation potentials of CH, HK2, and THNM2
587 after ozonation was effectively offset by biodegradation at typical contact times regardless
588 of the initial concentration of precursors in the influent.
589 • The dynamics of removal of DOC and DBP formation potentials by biofiltration at different
590 EBCTs followed first-order reaction kinetics with a plateau of residual biorecalcitrant
591 concentration attained after approximately 10-20 min of EBCT. This study highlighted the
592 importance of EBCT as a key design parameter for biofiltration. The experimentally

593 determined rate constants may be useful in prediction of DBP formation potential reductions
594 and determine the EBCT required to attain a target DBP concentration in the treated
595 drinking water.

596 • The reduction in DBP formation potentials varied with respect to species, indicating the
597 influence of DBP precursor structure and reactivity on biodegradability. The measured rate
598 constants of DBP formation potential before reaching the steady-state concentration
599 followed this order: CH > HK2 ≈ THNM2 > HAN4 > THM4> TCAM > HAA8.

600 • Due to the increase in bromide to DOC ratio after ozonation and biofiltration, the
601 concentrations of bromine-containing DBPs (e.g., TBM, DBAN, TBNM) increased after
602 these sequential treatments followed by chlorination. Thus, conditions promoting strong
603 DOC removal such as longer EBCTs (e.g., > 20 min) can promote the formation of
604 bromine-containing DBPs in bromide-containing waters. Treatment engineers should take
605 this risk into account on a case-by-case basis.

606

607 **Acknowledgements**

608 This study was funded by Seqwater (Australia) and the Water Research Foundation (project
609 WRF #4484). Glen De Vera would like to thank the Australia Awards PhD scholarship. Dr. Maria
610 José Farré acknowledges the European Commission for funding project 623711 under the FP7-
611 PEOPLE-2013-IIF - Marie Curie Action: "International Incoming Fellowships" and Dr Wolfgang
612 Gernjak acknowledges funding obtained from the Spanish Government for a Ramon y Cajal
613 Research Fellowship (RYC-2012-12181). Thanks also to Deb Gale and other Seqwater staff who
614 were involved in the sampling at treatment plants and Dr. Kalinda Watson for her assistance in
615 AOX analysis. Peng Liu is also acknowledged for useful discussions. We appreciate the careful
616 revision and constructive comments provided by the reviewers.

617

618

619

620

621 **References**

622 Bader, H., Sturzengger, V. and Hoigne, J. (1988) Photometric method for the determination of low
623 concentrations of hydrogen peroxide by the peroxidase catalyzed oxidation of N,N-diethyl-p-
624 phenylenediamine (DPD). Water Res. 22(9), 1109-1115.
625 Black, K.E. and Berube, P.R. (2014) Rate and extent NOM removal during oxidation and
626 biofiltration. Water Res. 52, 40-50.
627 Carlson, K.H. and Amy, G.L. (1998) BOM removal during biofiltration. J. Am. Water Works Ass.
628 90(12), 42-52.
629 Chon, K., Salhi, E. and von Gunten, U. (2015) Combination of UV absorbance and electron
630 donating capacity to assess degradation of micropollutants and formation of bromate during
631 ozonation of wastewater effluents. Water Res. 81, 388-397.
632 Chu, W., Gao, N., Yin, D., Deng, Y. and Templeton, M.R. (2012) Ozone-biological activated
633 carbon integrated treatment for removal of precursors of halogenated nitrogenous disinfection
634 by-products. Chemosphere 86(11), 1087-1091.
635 Criegee, R. (1975) Mechanisms of ozonolysis. Angew Chem 87(765-771).
636 De Vera, G.A.D., Stalter, D., Gernjak, W., Weinberg, H.S., Keller, J. and Farre, M.J. (2015)
637 Towards reducing DBP formation potential of drinking water by favouring direct ozone over
638 hydroxyl radical reactions during ozonation. Water Res. 87, 49-58.
639 Doederer, K., Gernjak, W., Weinberg, H.S. and Farre, M.J. (2014) Factors affecting the formation
640 of disinfection by-products during chlorination and chloramination of secondary effluent for the
641 production of high quality recycled water. Water Res. 48, 218-228.

642 Domino, M.M., Pepich, B.V., Munch, D.J., Fair, P.S. and Xie, Y. (2003) US EPA Method 552.3.
643 Determination of haloacetic acids and dalapon in drinking water by liquid-liquid
644 microextraction, derivatization, and gas chromatography with electron capture detection. EPA
645 815-B-03-002. US EPA, Cincinnati, OH, USA.
646 Elovitz, M.S. and von Gunten, U. (1999) Hydroxyl radical/ozone ratios during ozonation processes.
647 I. the Rct concept. Ozone-Sci. Eng. 21(3), 239-260.
648 Evans, P.J., Smith, J.L., LeChevallier, M.W., Schneider, O.D., Weinrich, L.A. and Jjemba, P.K.
649 (2013) Biological filtration monitoring and control toolbox: Guidance manual. Water Research
650 Foundation, CO, USA.
651 Farré, M.J., Day, S., Neale, P.A., Stalter, D., Tang, J.Y. and Escher, B.I. (2013) Bioanalytical and
652 chemical assessment of the disinfection by-product formation potential: role of organic matter.
653 Water Res. 47(14), 5409-5421.
654 Farré, M.J., Lyon, B., de Vera, G.A., Stalter, D. and Gernjak, W. (2016) Assessing adsorbable
655 organic halogen formation and precursor removal during drinking water production. J.Environ.
656 Eng. 142(3), 04015087.
657 Gagnon, G.A., Booth, S.D.J., Peldszus, S., Mutti, D., Smith, F. and Huck, P.M. (1997) Carboxylic
658 acids: formation and removal in full-scale plants. J. Am .Water Works Ass. 89(8), 88-97.
659 Gagnon, G.A. and Huck, P.M. (2001) Removal of easily biodegradable organic compounds by
660 drinking water biofilms: analysis of kinetics and mass transfer. Water Res. 35(10), 2254-2564.
661 Gao, J., Ellis, L.B.M. and Wacket, L.P. (2010) The University of Minnesota
662 biocatalysis/biodegradation database: improving public access. Nucleic Acids Res. 38, D488-
663 D491.
664 Glezer, V., Harris, B., Tal, N., Iosefvon, B. and Lev, O. (1999) Hydrolysis of haloacetonitriles:
665 Linear free energy relationship, kinetics and products. Water Res. 33(8), 1938-1948.

666 Gruchlik, Y., Heitz, A., Tan, J., Sebastien, A., Bowman, M., Halliwell, D., von Gunten, U., J., C.
667 and Joll, C. (2014) Impact of bromide and iodide during drinking water disinfection and
668 potential treatment processes for their removal or mitigation. Water: J. Aust. Water Ass. 41(8),
669 38-43.
670 Hammes, F., Salhi, E., Koster, O., Kaiser, H.P., Egli, T. and von Gunten, U. (2006) Mechanistic
671 and kinetic evaluation of organic disinfection by-product and assimilable organic carbon (AOC)
672 formation during the ozonation of drinking water. Water Res. 40(12), 2275-2286.
673 Heeb, M.B., Criquet, J., Zimmermann-Steffens, S.G. and von Gunten, U. (2014) Oxidative
674 treatment of bromide-containing waters: formation of bromine and its reactions with inorganic
675 and organic compounds-a critical review. Water Res. 48, 15-42.
676 Hua, G. and Reckhow, D.A. (2007a) Characterization of disinfection byproduct precursors based on
677 hydrophobicity and molecular size. Environ. Sci. Technol. 41, 3309-3315.
678 Hua, G. and Reckhow, D.A. (2007b) Comparison of disinfection byproduct formation from chlorine
679 and alternative disinfectants. Water Res. 41(8), 1667-1678.
680 Hua, G. and Reckhow, D.A. (2013) Effect of pre-ozonation on the formation and speciation of
681 DBPs. Water Res. 47(13), 4322-4330.
682 Huang, H., Wu, Q.Y., Hu, H.Y. and Mitch, W.A. (2012) Dichloroacetonitrile and
683 dichloroacetamide can form independently during chlorination and chloramination of drinking
684 waters, model organic matters, and wastewater effluents. Environ. Sci. Technol. 46(19), 10624-
685 10631.
686 Hubner, U., von Gunten, U. and Jekel, M. (2015) Evaluation of the persistence of transformation
687 products from ozonation of trace organic compounds - a critical review. Water Res. 68, 150-170.
688 Huck, P.M. and Sozanski, M.M. (2008) Biological filtration for membrane pre-treatment and other
689 applications: towards the development of a practically-oriented performance parameter. J. Water
690 Supply Res. Technol.-Aqua 57(4), 203.

691 Huck, P.M., Zhang, S. and Price, M.L. (1994) BOM removal during biological treatment: a first-
692 order model. J. Am. Water Works Ass. 86(6), 61-71.
693 Juhna, T. and Melin, E. (2006) Ozonation and biofiltration in water treatment - operational status
694 and optimization issues. Techneau. Available at
695 http://www.techneau.org/fileadmin/files/Publications/Publications/Deliverables/D5.3.1B-
696 OBF.pdf.
697 Krasner, S.W. (2009) The formation and control of emerging disinfection by-products of health
698 concern. Philos. Trans. A Math. Phys. Eng. Sci. 367(1904), 4077-4095.
699 Liang, L. and Singer, P.C. (2003) Factors influencing the formation and relative distribution of
700 haloacetic acids and trihalomethanes in drinking water. Environ. Sci. Technol. 37(13), 2920-
701 2928.
702 Liao, X., Zou, R., Chen, C., Yuan, B., Zhou, Z., Ma, H. and Zhang, X. (2016) Biomass
703 development in GAC columns receiving influents with different levels of nutrients. Water Sci.
704 Technol. Water Supply 16(4), 1024-1032.
705 Lyon, B.A., Farre, M.J., De Vera, G.A., Keller, J., Roux, A., Weinberg, H.S. and Gernjak, W.
706 (2014) Organic matter removal and disinfection byproduct management in South East
707 Queensland's drinking water. Water Sci. Technol. Water Supply 14(4), 681-689.
708 McCurry, D.L., Quay, A.N. and Mitch, W.A. (2016) Ozone Promotes Chloropicrin Formation by
709 Oxidizing Amines to Nitro Compounds. Environ. Sci. Technol. 50(3), 1209-1217.
710 Melin, E.S. and Odegaard, H. (2000) The effect of biofilter loading rate on the removal of organic
711 ozonation by-products. Water Res. 34(18), 4464-4476.
712 Mitch, W.A., Krasner, S.W., Westerhoff, P. and Dotson, A. (2009) Occurrence and formation of
713 nitrogenous disinfection by-products. Water Research Foundation, CO, USA.
714 NATA (2013) Technical note 17-Guidelines for validation and verification of quantitative and
715 qualitative test methods. Available at:

http://www.nata.com.au/nata/phocadownload/publications/Guidance_information/tech-notes-information-papers/technical_note_17.pdf.

Nishijima, W. and Speitel, G.E. (2004) Fate of biodegradable dissolved organic carbon produced by ozonation on biological activated carbon. Chemosphere 56, 113-119.

Nogueira, R.F., Oliveira, M.C. and Paterlini, W.C. (2005) Simple and fast spectrophotometric determination of H_2O_2 in photo-Fenton reactions using metavanadate. Talanta 66(1), 86-91.

Nothe, T., Fahlenkamp, H. and von Sonntag, C. (2009) Ozonation of wastewater: Rate of ozone consumption and hydroxyl radical yield. Environ. Sci. Technol. 43(5990-5995).

Persson, F., Heinicke, G., Hedberg, T., Hermansson, M. and Uhl, W. (2007) Removal of geosmin and MIB by biofiltration--an investigation discriminating between adsorption and biodegradation. Environ. Technol. 28(1), 95-104.

Pipe-Martin, C. (2008) Dissolved organic carbon removal by biological treatment. WIT Transactions on Ecology and the Environment 111, 445-452. http://www.witpress.com/, ISSN 1743-3541 (on-line).

Plewa, M.J., Wagner, E.D., Muellner, M.G., Hsu, K.-M. and Richardson, S.D. (2008) Comparative mammalian cell toxicity of N-DBPs and C-DBPs. Symposium Series 995. In: Karanfil,Tanju, Krasner, Stuart, W., Westerhoff, Paul, Xie, Yuenfeng (Eds.), Disinfection by-products in drinking water: Occurrence, formation, health effect, and control. Washington, District of Columbia, US, American Chemical Society, pp. 36–50.

Ramseier, M.K., Peter, A., Traber, J. and von Gunten, U. (2011) Formation of assimilable organic carbon during oxidation of natural waters with ozone, chlorine dioxide, chlorine, permanganate, and ferrate. Water Res. 45(5), 2002-2010.

Ramseier, M.K. and von Gunten, U. (2009) Mechanisms of phenol ozonation—Kinetics of formation of primary and secondary reaction products. Ozone-Sci. Eng. 31(3), 201-215.

740 Rattier, M., Reungoat, J., Keller, J. and Gernjak, W. (2014) Removal of micropollutants during
741 tertiary wastewater treatment by biofiltration: Role of nitrifiers and removal mechanisms. Water
742 Res. 54, 89-99.
743 Reckhow, D.A. and Singer, P.C. (1984) The removal of organic halide precursors by preozonation
744 and alum coagulation. J. Am. Water Works Ass. 76(4), 151-157.
745 Richardson, S.D. (2003) Disinfection by-products and other emerging contaminants in drinking
746 water. TrAC - Trends Anal. Chem. 22(10), 666-684.
747 Rittman, B.E., Bae, W., Namkung, E. and Lu, C.-J. (1987) A critical evaluation of microbial
748 product formation in biological processes. Water Sci. Technol. 19(3-4), 517-528.
749 Sarathy, S.R. (2004) Effects of UV/H2O2 advanced oxidation on physical and chemical
750 characteristics of natural organic matter in raw drinking water sources. PhD thesis. University of
751 British Columbia, Vancouver, Canada.
752 Sedlak, D.L. and von Gunten, U. (2011) The chlorine dilemma. Science 331(6013), 42-43.
753 Singer, P.C., Obolensky, A. and Greiner, A. (1995) DBPs in chlorinated North Carolina drinking
754 waters. J. Am. Water Works Ass. 87(10), 83-92.
755 Speitel, G.E.J., Symons, J.M., Diehl, A.C., Sorensen, H.W. and Cipparone, L.A. (1993) Effect of
756 ozone dosage and subsequent biodegradation on removal of DBP precursors. J. Am. Water
757 Works Ass. 85(5), 86-95.
758 Stalter, D., Peters, L., O'Malley, E., Tang, J.Y., Revalor, M., Farre, M.J., Watson, K., von Gunten,
759 U. and Escher, B.I. (2016) Sample enrichment for bioanalytical assessment of disinfected
760 drinking water: concentrating the polar, the volatiles, the unknowns. Environ. Sci. Technol.
761 50(12), 6495-6505.
762 Symons, J.M., Krasner, S.W., Simms, L.A. and Sclimenti, M. (1993) Measurement of THM and
763 precursor concentrations revisited: The effect of bromide ion. J. Am. Water Works Ass. 85(1),
764 51-62.

765 Urfer, D., Huck, P.M., Booth, S.D.J. and Coffey, B.M. (1997) Biological filtration for BOM and
766 particle removal: a critical review. J. Am. Water Works Ass. 18(12), 83-98.
767 USEPA (2010) 40 CFR Appendix B to part 136 - Definition and procedure for determination of the
768 method detection limit - revision 1.11. Available at: https://www.gpo.gov/fdsys/pkg/CFR-2012-
769 title40-vol24/pdf/CFR-2012-title40-vol24-part136-appB.pdf.
770 von Gunten, U. (2003) Ozonation of drinking water: Part I. Oxidation kinetics and product
771 formation. Water Res. 37(7), 1443-1467.
772 von Sonntag, C. and von Gunten, U. (2012) Chemistry of ozone in water and wastewater treatment -
773 from basic principles to applications. IWA Publishing, London, UK.
774 Wadhawan, T., Simsek, H., Kasi, M., Knutson, K., Prubeta, B., McEvoy, J. and Khan, E. (2014)
775 Dissolved organic nitrogen and its biodegradable portion in a water treatment plant with ozone
776 oxidation. Water Res. 54, 318-326.
777 Weinberg, H.S., Glaze, W.H., Krasner, S.W. and Sclimenti, M.J. (1993) Formation and removal of
778 aldehydes in plants that use ozonation. J. Am. Water Works Ass. 85(5), 72-85.
779 Wenk, J., Aeschbacher, M., Salhi, E., Canonica, S., von Gunten, U. and Sander, M. (2013)
780 Chemical oxidation of dissolved organic matter by chlorine dioxide, chlorine, and ozone: effects
781 on its optical and antioxidant properties. Environ. Sci. Technol. 47(19), 11147-11156.
782 Westerhoff, P., Chao, P. and Mash, H. (2004) Reactivity of natural organic matter with aqueous
783 chlorine and bromine. Water Res. 38(6), 1502-1513.
784 Yavich, A.A., Lee, K.H., Chen, K.C., Pape, L. and Masten, S.J. (2004) Evaluation of
785 biodegradability of NOM after ozonation. Water Res. 38(12), 2839-2846.
786 Yeh, R.Y., Farre, M.J., Stalter, D., Tang, J.Y., Molendijk, J. and Escher, B.I. (2014) Bioanalytical
787 and chemical evaluation of disinfection by-products in swimming pool water. Water Res. 59,
788 172-184.

789

Figure Captions:

Fig. 1. Impact of chlorination, ozonation, and biodegradation on DBP precursors: (a) phenolates, (b) olefins, and (c) amines. Biotransformation rules were taken from the University of Minnesota Biocatalysis/Biodegradation Database (https://umbbd.ethz.ch/) (Gao et al. 2010). THMs = trihalomethanes, HAAs = haloacetic acids, CH = chloral hydrate, HK = haloketones, HANs = haloacetonitriles, TCAM = trichloroacetamide, THNM = trihalonitromethanes. Reactions were based on the following references: Deborde and von Gunten (2008), Hubner et al. (2015), McCurry et al. (2016), Wenk et al. (2013), Ramseier and von Gunten (2009), von Sonntag and von Gunten (2012).

Fig. 2. Effect of batch biodegradation (O_3+AN) on water samples ozonated (O_3) at different doses on (a) dissolved organic carbon (DOC) and formation potentials of (b) trihalomethanes (THM4), (c) chloral hydrate (CH), (d) haloketones (HK2), (e) haloacetonitriles (HAN4), (f) trihalonitromethanes (THNM2), and (g) trichloroacetamide (TCAM). Conditions: Sample/bioactive anthracite (volume/mass) = 500 mL/170g; contact time = 7 days; pH = 7; temperature = 22 ± 1 ^{0}C, chlorine residual = 3.4 ± 0.9 mg/L as Cl_2. "No O3" represents formation potentials of non-ozonated samples. Error bars depict mean absolute deviation obtained from experiment (n=1) with 2 DBP extractions per sample. C_0 = contaminant concentration before ozonation and biodegradation, C = contaminant concentration after treatment.

Fig. 3. Effect of ozonation and biofiltration with anthracite (AN) and activated carbon (BAC) media on (a) dissolved organic carbon (DOC) and formation potentials of (b) trihalomethanes (THM4), (c) chloral hydrate (CH), (d) haloketones (HK2), (e) haloacetonitriles (HAN4), (f) trihalonitromethanes (THNM2), (g) trichloroacetamide (TCAM), and (h) adsorbable organic halogen (AOX). Conditions: transferred O_3 dose = 1.2 mgO_3/mgDOC; bed volume = 7 mL; empty bed contact time

= 11 min, pH = 7; temperature = 22 ± 1 ^{0}C; chlorine residual = 1.5 ± 0.6 mg/L as Cl_2. Error bars depict mean absolute deviation of experiments (n=2, with 2 DBP extractions per sample; for AOX, n=1). C_0 = contaminant concentration before ozonation and biodegradation, C = contaminant concentration after treatment.

Fig. 4. Changes in (a) dissolved organic carbon (DOC) and formation potentials post-chlorination of (b) trihalomethanes (THM4), (c) haloacetic acids (HAA8), (d) chloral hydrate (CH), (e) haloketones (HK2), (f) haloacetonitriles (HAN4), (g) trihalonitromethanes (THNM), (h) trichloroacetamide (TCAM), and (i) adsorbable organic halogen (AOX) as a result of O_3/H_2O_2 treatment and subsequent column biofiltration with anthracite (AN), and biological activated carbon (BAC). Conditions: transferred ozone dose = 1 mg/mg DOC mg/L; bed volume = 7 mL; empty bed contact time = 11 min, pH = 7; influent DO = 11.5 ± 0.7 mg/L; effluent DO = 6.6 ± 0.2 mg/L; temperature = 22 ± 1 ^{0}C; chlorine residual = 1 – 2.7 mg/L as Cl_2. "No O_3" at x-axis are formation potentials of non-ozonated samples. Error bars depict mean absolute deviation of experiments (BAC: n=2, AN: n=1, with 2 DBP extractions per sample; for HAA, n=1). n.a. = no test done at the specific experimental condition.

Fig. 5. Effect of biofiltration EBCT on changes in (a) DOC and formation potentials of (b) trihalomethanes (THM4), (c) haloacetic acids (HAA8), (d) chloral hydrate (CH), (e) haloketones (HK2), (f) haloacetonitriles (HAN4), (g) trihalonitromethanes (THNM2), (h) trichloroacetamide (TCAM), and (i) adsorbable organic halogen (AOX) of ozonated water sample. Conditions: transferred ozone dose = 1 mg/mg DOC, DOC = 15 mg/L, bromide = 300 μg/L, bed volume = 12 mL, media = BAC, pH = 6.9, temperature = 22 ± 1 ^{0}C, chlorine residual = 3.1 ± 0.8 mg/L as Cl_2. The symbols are the experimental data, broken lines correspond to formation potentials measured without ozonation, and solid lines present model fits (single exponential decay to P_f). Residuals from the model fit shows a normal distribution (P values > 0.05, Shapiro-Wilk test, last point for

ACCEPTED MANUSCRIPT

THNM2 and HAN4 not included). Error bars depict standard deviation of 3 replicate experiments (with 2 DBP extractions per sample).

ACCEPTED MANUSCRIPT

Table 1. Model parameters for reduction in DBP formation potentials after BAC filtration of ozonated water samples[a]

DBP	P_f[b], μM	P_{biodeg}[c], μM	k[d], min^{-1}	R^2[e]	$S_{y\|x}$[f]	n[g]
THM4	1.45 ± 0.04	1.22 ± 0.09	0.28 ± 0.05	0.9657	0.0840	10
HAA8	0.69 ± 0.06	0.93 ± 0.10	0.15 ± 0.04	0.9688	0.0860	6
CH	0.074 ± 0.004	0.284 ± 0.012	0.58 ± 0.07	0.9877	0.0113	10
HK2	0.068 ± 0.003	0.176 ± 0.009	0.50 ± 0.07	0.9808	0.0087	10
HAN4	0.068 ± 0.001	0.037 ± 0.002	0.33 ± 0.04	0.9844	0.0018	9
THNM2	0.0171 ± 0.0002	0.0597 ± 0.0006	0.48 ± 0.01	0.9993	0.0006	9
TCAM	0.0050 ± 0.0002	0.0046 ± 0.0004	0.16 ± 0.03	0.9561	0.0004	10
AOX	12.86 ± 0.34	13.03 ± 0.46	0.11 ± 0.01	0.9904	0.5113	11
DOC	10.14 ± 0.17[h]	3.57 ± 0.38[h]	0.26 ± 0.06	0.9268	0.3646	10
Cl_2 demand	3.77 ± 0.13[h]	3.03 ± 0.23[h]	0.13 ± 0.02	0.9621	0.2272	10

[a]obtained from non-linear regression (SigmaPlot 13.0); [b]P_f = final steady state concentration (EBCT > 20 min); [c]P_{biodeg}= DBP formation potential from influent - P_f; [d]k = specific first-order rate constant; [e]R^2 = coefficient of determination; [f]$S_{y|x}$ (standard error of the estimate) = $(SS/df)^{1/2}$ where SS is the sum-of-squares of the distance of the linear regression from the data points and df is the degrees of freedom (i.e. n-2); [g]n = number of data points (each data point is the average of 3 replicate experiments); [h]units = mg/L as C for DOC and as Cl_2 for chlorine demand.

ACCEPTED MANUSCRIPT

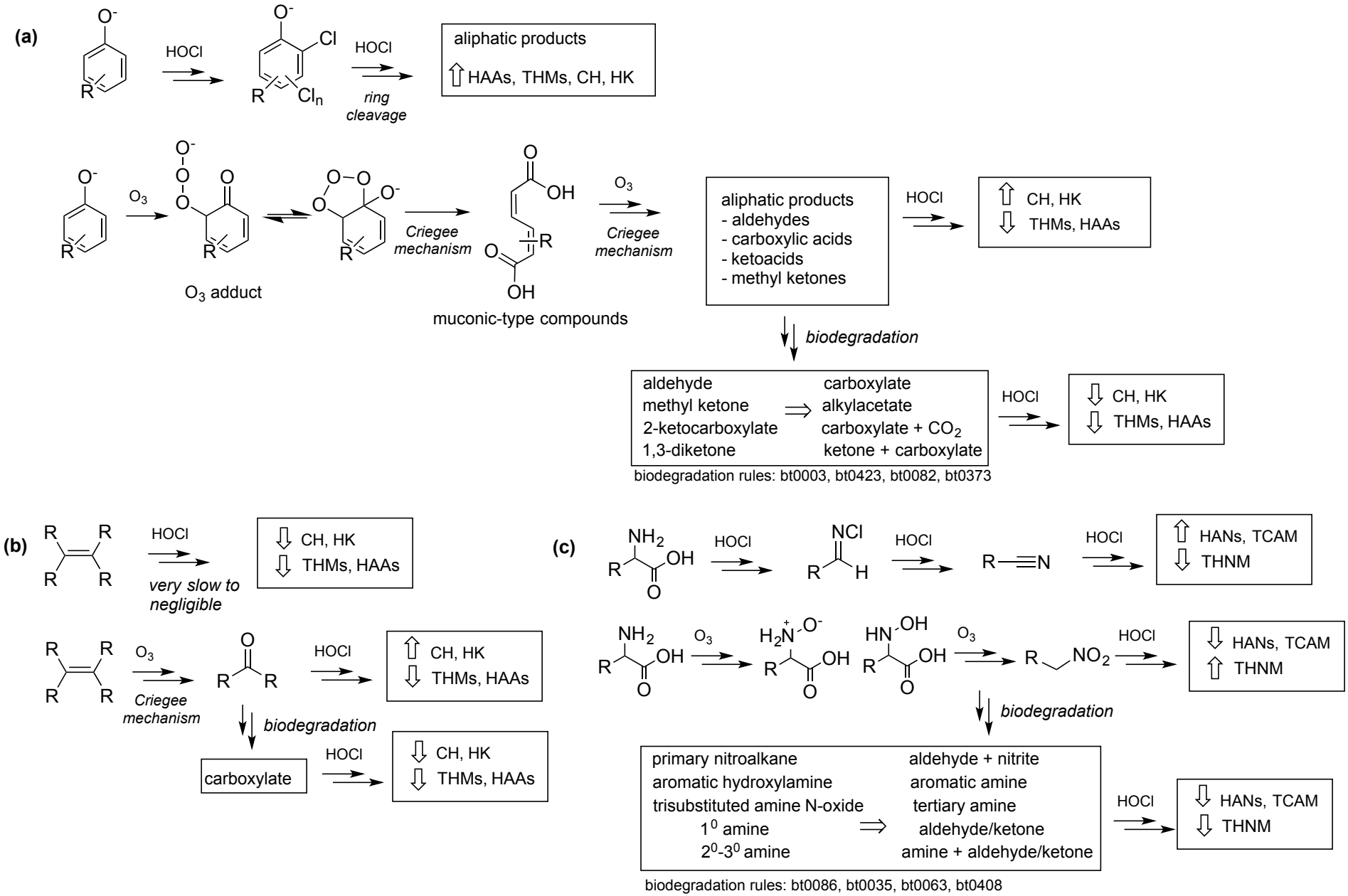
(a)
HOCl
HOCl
ring cleavage
aliphatic products
⇧ HAAs, THMs, CH, HK
O3
O3 adduct
Criegee mechanism
muconic-type compounds
O3
Criegee mechanism
aliphatic products
- aldehydes
- carboxylic acids
- ketoacids
- methyl ketones
HOCl
⇧ CH, HK
⇩ THMs, HAAs
biodegradation
aldehyde ⟹ carboxylate
methyl ketone ⟹ alkylacetate
2-ketocarboxylate ⟹ carboxylate + CO2
1,3-diketone ⟹ ketone + carboxylate
HOCl
⇩ CH, HK
⇩ THMs, HAAs
biodegradation rules: bt0003, bt0423, bt0082, bt0373
(b)
HOCl
very slow to negligible
⇩ CH, HK
⇩ THMs, HAAs
O3
Criegee mechanism
HOCl
⇧ CH, HK
⇩ THMs, HAAs
biodegradation
carboxylate
HOCl
⇩ CH, HK
⇩ THMs, HAAs
(c)
HOCl
HOCl
HOCl
⇧ HANs, TCAM
⇩ THNM
O3
O3
HOCl
⇩ HANs, TCAM
⇧ THNM
biodegradation
primary nitroalkane ⟹ aldehyde + nitrite
aromatic hydroxylamine ⟹ aromatic amine
trisubstituted amine N-oxide ⟹ tertiary amine
1⁰ amine ⟹ aldehyde/ketone
2⁰-3⁰ amine ⟹ amine + aldehyde/ketone
HOCl
⇩ HANs, TCAM
⇩ THNM
biodegradation rules: bt0086, bt0035, bt0063, bt0408

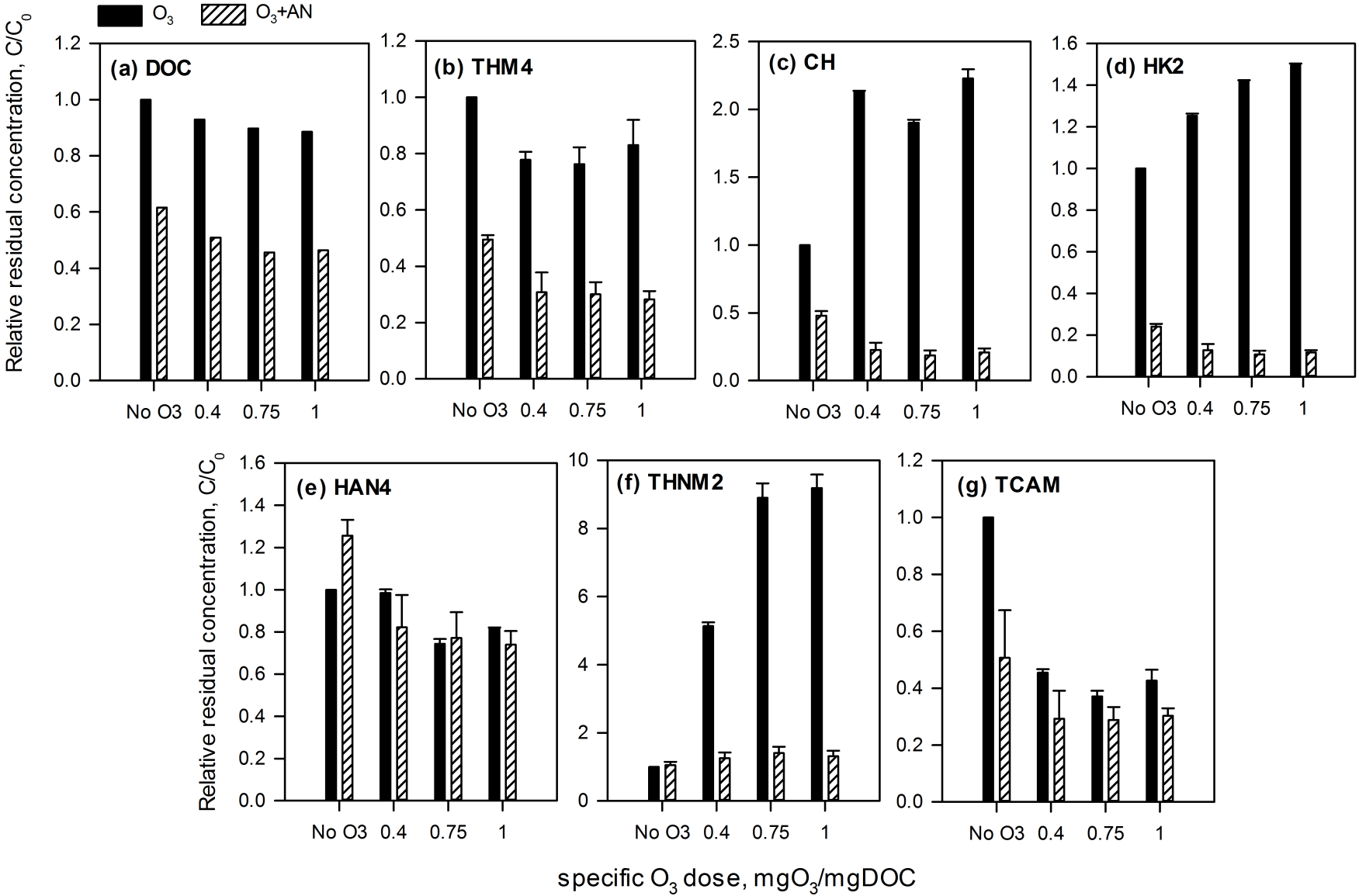
O3
O3+AN
Relative residual concentration, C/C0
(a) DOC
(b) THM4
(c) CH
(d) HK2
(e) HAN4
(f) THNM2
(g) TCAM
No O3
0.4
0.75
1
specific O3 dose, mgO3/mgDOC

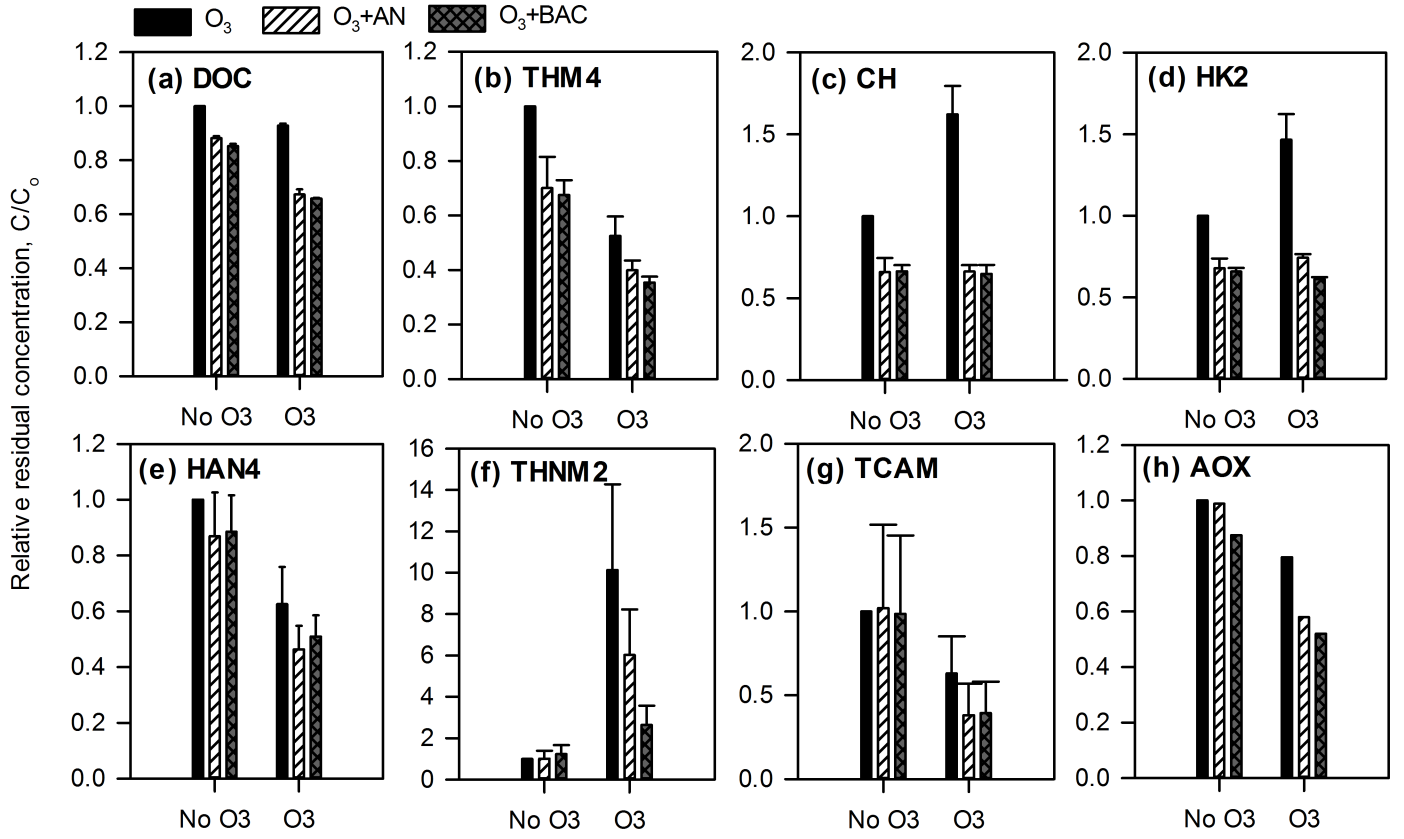
O3
O3+AN
O3+BAC
Relative residual concentration, C/Co
(a) DOC
(b) THM4
(c) CH
(d) HK2
(e) HAN4
(f) THNM2
(g) TCAM
(h) AOX
No O3
O3

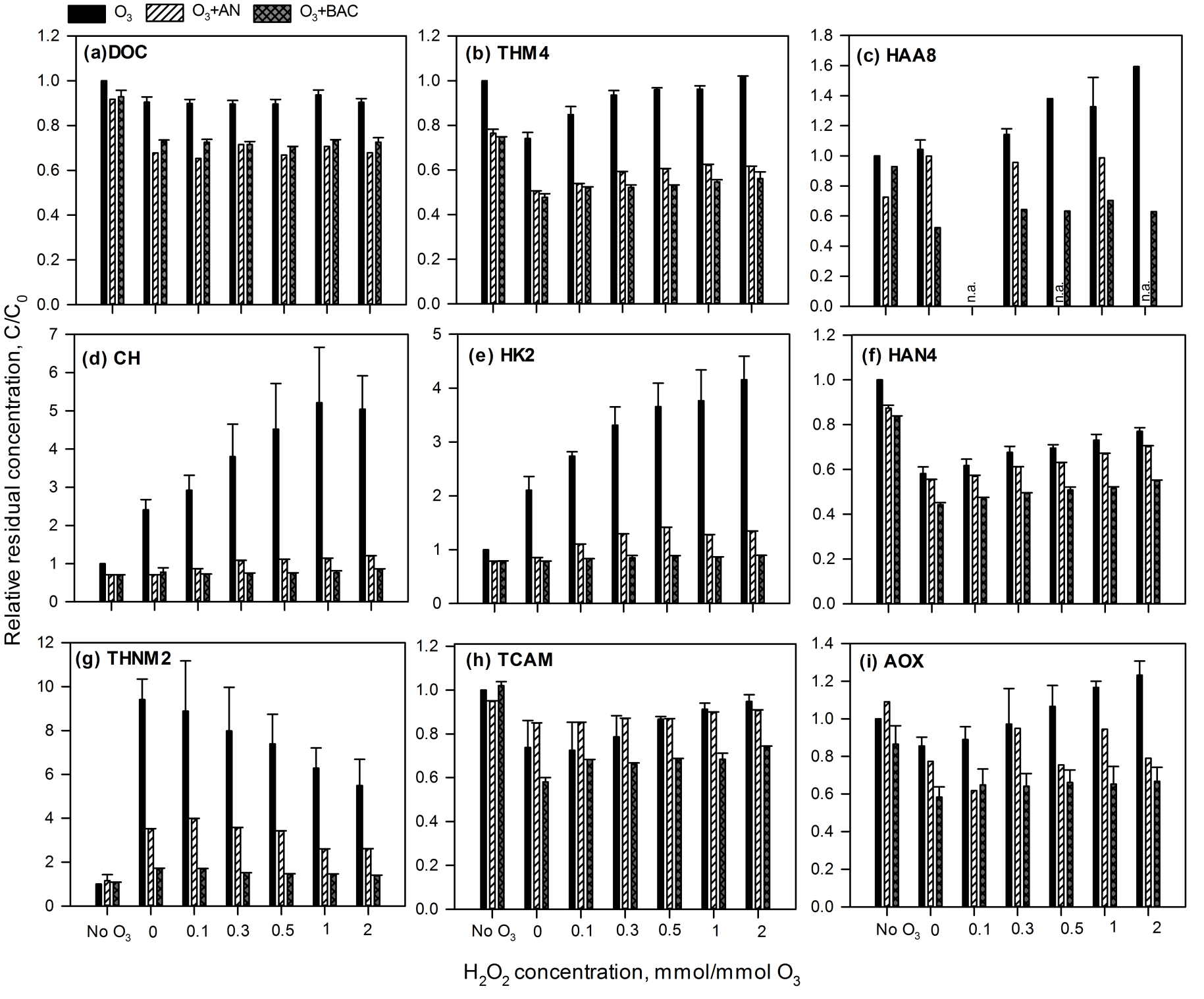
O3
O3+AN
O3+BAC
(a)DOC
(b) THM4
(c) HAA8
(d) CH
(e) HK2
(f) HAN4
(g) THNM2
(h) TCAM
(i) AOX
n.a.
Relative residual concentration, C/C0
No O3
0
0.1
0.3
0.5
1
2
H2O2 concentration, mmol/mmol O3

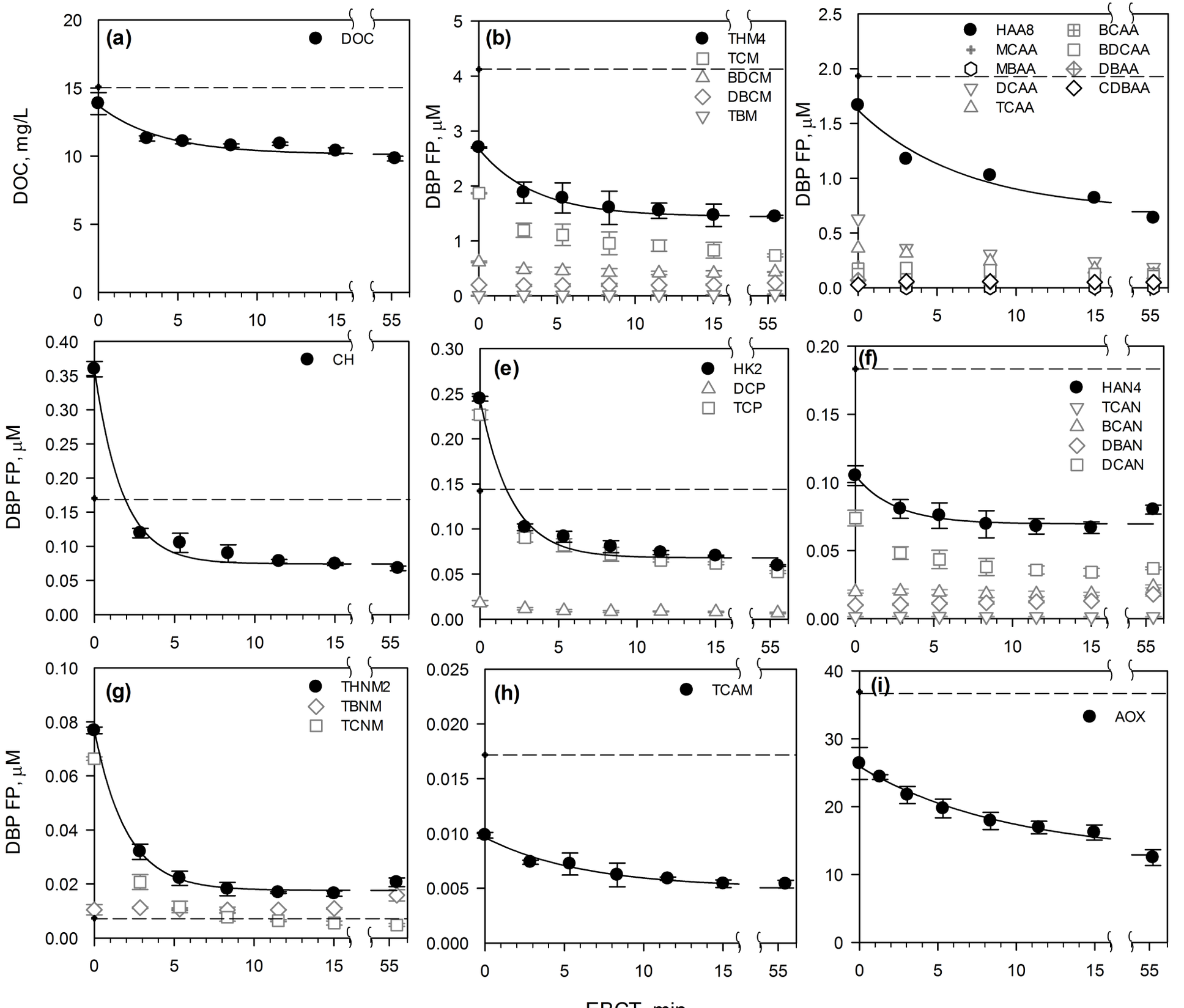
(a)
DOC
DOC, mg/L
(b)
THM4
TCM
BDCM
DBCM
TBM
DBP FP, μM
HAA8
MCAA
MBAA
DCAA
TCAA
BCAA
BDCAA
DBAA
CDBAA
DBP FP, μM
CH
DBP FP, μM
(e)
HK2
DCP
TCP
(f)
HAN4
TCAN
BCAN
DBAN
DCAN
(g)
THNM2
TBNM
TCNM
DBP FP, μM
(h)
TCAM
(i)
AOX
EBCT, min

ACCEPTED MANUSCRIPT

Highlights

- Biofiltration reduces DBP FP with 1st-order dependence on filter contact time.
- NOM removal by biofiltration increases Br substitution in subsequent disinfection.
- Combined O_3 + biofiltration (EBCT: 10-20 min) effectively controlled DBP formation.
- DBP precursor removal by BAC was highest for CH, THNM2, and HK2.
- Biofiltration attenuates effects of varying O_3 exposures on DBP formation.

ACCEPTED MANUSCRIPT